Published February 21, 2011

Thymic stromal lymphopoietin fosters human breast tumor growth by promoting type 2 inflammation

Alexander Pedroza-Gonzalez,[1] Kangling Xu,[1,2] Te-Chia Wu,[1,2] Caroline Aspord,[1] Sasha Tindle,[1] Florentina Marches,[1] Michael Gallegos,[1] Elizabeth C. Burton,[4] Daniel Savino,[4] Toshiyuki Hori,[5] Yuetsu Tanaka,[6] Sandra Zurawski,[1] Gerard Zurawski,[1] Laura Bover,[7] Yong-Jun Liu,[7] Jacques Banchereau,[1,8,9] and A. Karolina Palucka[1,3,8,9]

[1]Baylor Institute for Immunology Research, Baylor Research Institute, Dallas, TX 75204
[2]Department of Biomedical Studies, Baylor University, Waco, TX 76706
[3]Sammons Cancer Center, [4]Baylor University Medical Center, Dallas, TX 75246
[5]Department of Hematology and Oncology, Graduate School of Medicine, Kyoto University, Sakyoku, Kyoto 606-8507, Japan
[6]Department of Immunology, University of the Ryukyus, Okinawa 903-0215, Japan
[7]MD Anderson Cancer Center, Houston, TX 77030
[8]Department of Gene and Cell Medicine and [9]Department of Medicine, Immunology Institute, Mount Sinai School of Medicine, New York, NY 10029

The human breast tumor microenvironment can display features of T helper type 2 (Th2) inflammation, and Th2 inflammation can promote tumor development. However, the molecular and cellular mechanisms contributing to Th2 inflammation in breast tumors remain unclear. Here, we show that human breast cancer cells produce thymic stromal lymphopoietin (TSLP). Breast tumor supernatants, in a TSLP-dependent manner, induce expression of OX40L on dendritic cells (DCs). OX40L$^+$ DCs are found in primary breast tumor infiltrates. OX40L$^+$ DCs drive development of inflammatory Th2 cells producing interleukin-13 and tumor necrosis factor in vitro. Antibodies neutralizing TSLP or OX40L inhibit breast tumor growth and interleukin-13 production in a xenograft model. Thus, breast cancer cell–derived TSLP contributes to the inflammatory Th2 microenvironment conducive to breast tumor development by inducing OX40L expression on DCs.

CORRESPONDENCE
A. Karolina Palucka:
karolinp@baylorhealth.edu

Abbreviations used: HPC, hematopoietic progenitor cell; mDC, myeloid DC; NOD/SCID/β2m$^{-/-}$, nonobese diabetic/LtSz-scid/scid β2 microglobulin–deficient; TSLP, thymic stromal lymphopoietin.

There is accumulating evidence that inflammation plays a key role in the initiation and progression of cancer (Grivennikov et al., 2010). There are two types of inflammation that have opposing effects on tumors: (a) chronic inflammation, which promotes cancer cell survival and metastasis (Coussens and Werb, 2002; Condeelis and Pollard, 2006; Mantovani et al., 2008), and (b) acute inflammation, which can trigger cancer cell destruction as illustrated by regressions of bladder cancer after treatment with microbial preparations (Rakoff-Nahoum and Medzhitov, 2009). Although chronic inflammation is often linked with the presence of type 2–polarized macrophages (M2), acute inflammation associated with cancer destruction is linked with type 1–polarized macrophages (M1). M1 macrophages are induced by the type 1 cytokine IFN-γ, whereas, M2 macrophages are induced by the type 2 cytokines IL-4 and IL-13 (Mantovani and Sica, 2010).

Type 2 cytokines can contribute to tumorigenesis in several ways. For example, IL-13 produced by NKT cells induces myeloid cells to

A. Pedroza-Gonzalez's present address is Dept. of Gastroenterology and Hepatology, Erasmus MC, Rotterdam, Netherlands.
T.-C. Wu's present address is College of Life Sciences, Ritsumeikan University, Kusatsu, Shiga 525-8577, Japan.
C. Aspord's present address is Institut National de la Santé et de la Recherche Médicale U823, Immunobiology and Immunotherapy of Cancers, 38701, La Tronche, France.
J. Banchereau's present address is Hoffman-La Roche, Inc., Nutley, NJ.

© 2011 Pedroza-Gonzalez et al. This article is distributed under the terms of an Attribution–Noncommercial–Share Alike–No Mirror Sites license for the first six months after the publication date (see http://www.rupress.org/terms). After six months it is available under a Creative Commons License (Attribution–Noncommercial–Share Alike 3.0 Unported license, as described at http://creativecommons.org/licenses/by-nc-sa/3.0/).

The Journal of Experimental Medicine

Downloaded from jem.rupress.org on February 26, 2011

make TGF-β, which ultimately inhibits CTL functions (Berzofsky and Terabe, 2008). Spontaneous autochthonous breast carcinomas arising in Her-2/neu transgenic mice appear more quickly when the mice are depleted of T cells, which is evidence of T cell–mediated immunosurveillance slowing tumor growth (Park et al., 2008). This immunosurveillance could be further enhanced by blockade of IL-13, which slowed the appearance of these autologous tumors compared with control antibody-treated mice (Park et al., 2008). A spontaneous mouse breast cancer model recently highlighted the role of Th2 cells which facilitate the development of lung metastasis through macrophage activation (DeNardo et al., 2009). We identified $CD4^+$ T cells secreting IFN-γ and IL-13 in breast cancer tumors (Aspord et al., 2007). We also found that breast cancer cells express IL-13 on cell surface. Autocrine IL-13 has been shown to be important in the pathophysiology of Hodgkin's disease (Kapp et al., 1999; Skinnider et al., 2001, 2002). IL-13 and IL-13R are frequently expressed by Hodgkin's and Reed-Sternberg cells (Skinnider et al., 2001), and IL-13 stimulates their growth (Kapp et al., 1999; Trieu et al., 2004). Similar to Hodgkin's cells (Skinnider et al., 2002), breast cancer cells express pSTAT6 (Aspord et al., 2007), suggesting that IL-13 actually delivers signals to cancer cells. However, the mechanisms underlying the development of Th2 inflammation in breast cancer are unknown.

Like many other features of the immune response, Th1/Th2 polarization is regulated by DCs. In the steady state, nonactivated (immature) DCs present self-antigens to T cells, which leads to tolerance (Hawiger et al., 2001; Steinman et al., 2003). Once activated (mature), antigen-loaded DCs are geared toward the launching of antigen-specific immunity (Finkelman et al., 1996; Brimnes et al., 2003) leading to the proliferation of T cells and their differentiation into helper and effector cells. DCs are composed of distinct subsets, including myeloid DCs (mDCs) and plasmacytoid DCs (Caux et al., 1997; Maldonado-López et al., 1999; Pulendran et al., 1999; Luft et al., 2002; Dudziak et al., 2007; Klechevsky et al., 2008). DCs are also endowed with functional plasticity, i.e., they respond differentially to distinct activation signals (Steinman and Banchereau, 2007). For example, IL-10–polarized mDCs generate anergic $CD8^+$ T cells that are unable to lyse tumors (Steinbrink et al., 1999), as well as $CD4^+$ T cells with regulatory/suppressor function (Levings et al., 2005). In contrast, thymic stromal lymphopoietin (TSLP)–polarized mDCs are conditioned to express OX40 ligand (OX40L) and to expand T cells producing type 2 cytokines (Soumelis et al., 2002; Gilliet et al., 2003). Both the distinct DC subsets and their distinct response to microenvironment contribute to the generation of unique adaptive immune responses.

Unraveling the mechanisms by which breast cancer polarizes the immune responses might offer novel therapeutic options. This is important because despite declining mortality rates, breast cancer ranks second among cancer-related deaths in women. Worldwide, it is estimated that more than 1 million women are diagnosed with breast cancer every year, and >410,000 will die from the disease (Coughlin and Ekwueme, 2009). Here, we show that inflammatory Th2 cells that promote tumor development are driven by breast cancer–derived TSLP, which induces and maintains OX40L-expressing DCs in the tumor microenvironment. Thus, TSLP, and down-stream molecules, might represent novel potential therapeutic targets.

RESULTS

Inflammatory Th2 cells in primary breast cancer tumors

Our earlier study using a pilot cohort of 19 samples of primary breast cancer tumors revealed the secretion, upon activation with PMA and ionomycin, of both type 1 (IFN-γ) and type 2 (IL-4 and IL-13) cytokines (Aspord et al., 2007). The current study extends the analysis to a total of 99 consecutive samples (Table S1). Supernatants of activated tumor fragments display high levels of IFN-γ, IL-2, IL-4, IL-13, and TNF (Fig. 1 A and Table S1). Supernatants from tumor sites contained significantly higher levels of IL-2, type 2 (IL-4 and IL-13), and inflammatory (TNF) cytokines than those from macroscopically uninvolved surrounding tissue (Fig. 1 B and Table S1). Whereas a significant correlation can be observed between IL-2 levels in tumor and adjacent tissue ($P = 0.02$), IL-4 and IL-13 levels are not correlated ($P = 0.5$), further suggesting polarization of cytokine environment in breast tumors (Fig. 1 B). IFN-γ did not correlate with other cytokine levels (Table S1). However, levels of TNF were correlated with those of IL-13 ($P < 0.0001$; $r = 0.62$; $n = 98$) and IL-4 ($P = 0.0175$; $r = 0.31$; $n = 59$; Fig. 1 C). Thus, this survey of cytokine expression suggested Th2 polarization in the breast tumor microenvironment.

To identify the cells producing these cytokines, single-cell suspensions were prepared from tumors; activated for 5 h with PMA and ionomycin; stained with antibodies against T cells and cytokines; and analyzed by flow cytometry. Gated viable $CD4^+CD3^+$ T cells expressed IL-13 (3.67%), most of them coexpressing IFN-γ and TNF (Fig. 1 D and Fig. S1 A). A small fraction of $IL\text{-}13^+CD4^+$ T cells coexpressed IL-4, but none expressed IL-10 (Fig. 1 D). Such T cells have been referred to as inflammatory Th2 cells that are involved in allergic inflammatory diseases (Liu et al., 2007). Flow cytometry analysis of consecutive tumor infiltrates ($n = 22$) shows the overall increased percentages of IL-4– and IL-13–secreting $CD4^+CD3^+$ T cells ($P = 0.0313$ and $P = 0.0156$, respectively) when compared with adjacent tissue samples (Fig. 1 D and Fig. S1 B). Thus, the difference between tumor tissue and adjacent tissue appears to be caused by both the increased numbers of infiltrating T cells and enhanced polarization. The analysis of frozen tissue sections further demonstrated that infiltrating T cells in primary breast cancer tumors express IL-13 (Fig. 1 E). Thus, breast cancer tumors are infiltrated with inflammatory Th2 cells.

DCs infiltrating breast cancer tumors express OX40 ligand

Because OX40 ligation drives the differentiation of $CD4^+$ T cells into inflammatory Th2 (Ito et al., 2005), we analyzed the presence of OX40L in primary breast cancer tumors.

Downloaded from jem.rupress.org on February 26, 2011

Published February 21, 2011

Immunofluorescence staining of frozen tissue sections of primary breast cancer tumors showed the expression, in 57 out of 60 analyzed tumors, of OX40L by a majority of HLA-DR^{high} cells (Fig. 2 A). These OX40L^{+} cells are located in peritumoral areas (Fig. 2 A). Flow cytometry analysis of single-cell suspensions further confirmed the expression of OX40L by a fraction of HLA-DR^{high} CD14^{neg} CD11c^{high} mDCs (Fig. 2 B). Paired analysis demonstrated that the tumor beds express higher percentages of OX40L^{+} mDCs than the surrounding tissue (P = 0.0156; n = 7 paired samples; mean ± SE for surrounding tissue = 1.5 ± 0.8% [n = 7] and for breast cancer tumors 11 ± 1.67% [n = 12], respectively; Fig. 2 B). Thus, breast cancer tumors are infiltrated with OX40L^{+} mDCs.

Breast cancer tumors produce soluble factors that induce functional OX40L expression on DCs

To identify the breast cancer tumor factors that induce OX40L on mDCs, LIN^{neg}HLA-DR^{+} CD123^{-} CD11c^{+} mDCs were sorted from blood of healthy volunteers and

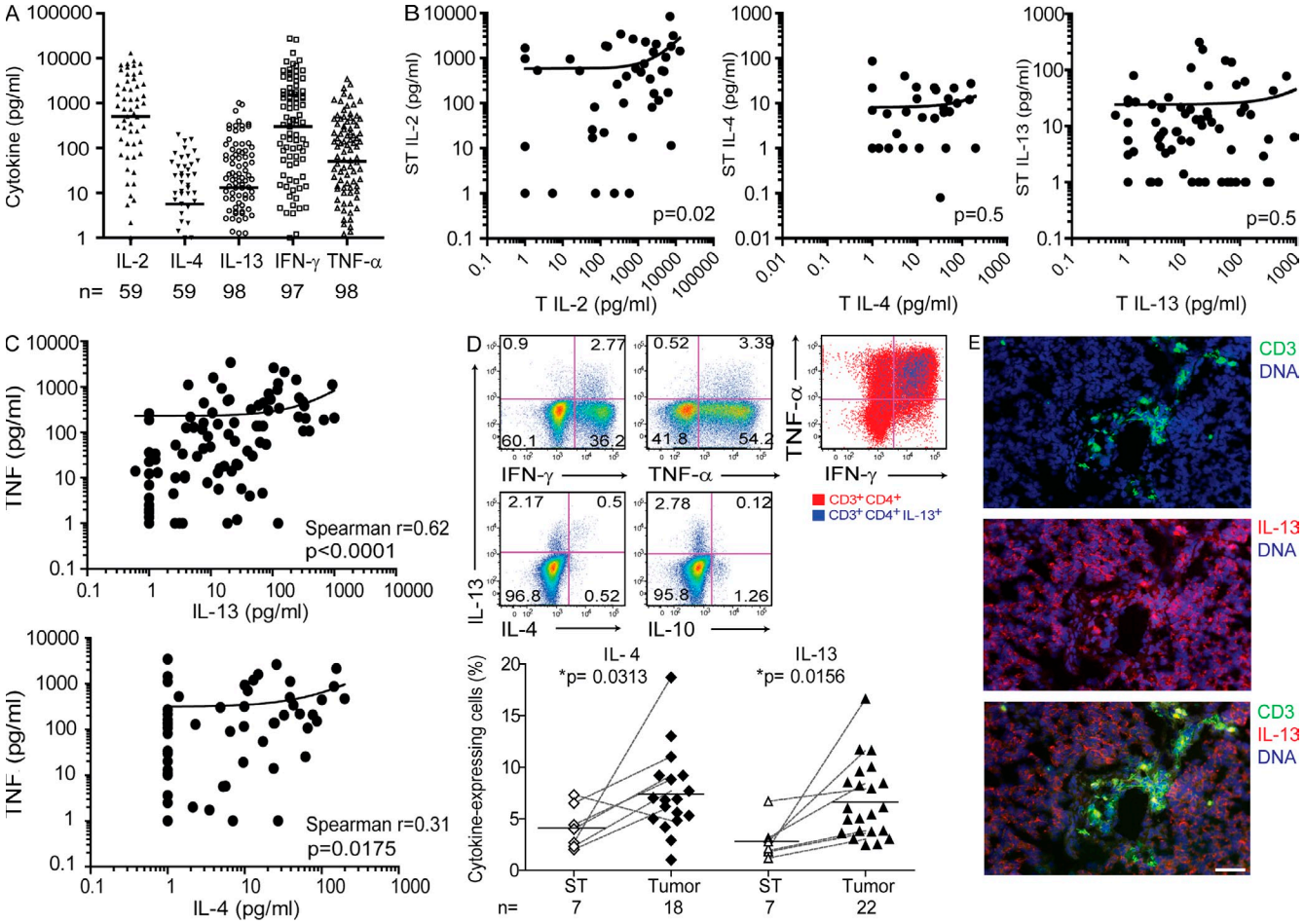

Figure 1. Inflammatory Th2 in breast cancer immune environment. (A) Cytokine profiles as determined by Luminex in supernatants of human breast tumor fragments stimulated for 16 h with PMA and ionomycin. Numbers on the x-axis indicate the number of tissue samples from different patients tested. (B) Cytokine profiles as determined by Luminex in supernatants of tumor fragments (T) and surrounding tissue (ST) from the same patient after PMA and ionomycin stimulation. Cytokine concentration values of IL-2, IL-4, and IL-13 from T and ST samples were plotted and analyzed using linear regression to determine the level of correlation between cytokine concentration in T and ST samples. (C) Cytokine profiles as determined by Luminex in supernatants of tumor fragments after PMA and ionomycin stimulation. Cytokine concentration values of TNF and IL-13 and of TNF and IL-4 were plotted and analyzed using nonparametric Spearman correlation to determine the level of correlation of two cytokines concentration in tumor samples. (D, top) Single-cell suspensions from tumor samples were stimulated for 5 h with PMA and ionomycin. Cytokine production was measured by flow cytometry. Dot plots are gated on CD3^{+}CD4^{+} T cells. (top right dot plot) Blue indicates gate on CD3^{+}CD4^{+}IL-13^{+} T cells that coexpress IFN-γ and TNF. Representative of four different patients from whom we have been able to obtain sufficient numbers of cells for 10-color analysis (patient nos. 148, 155, 164, and 169). Bottom, percentages of CD4^{+} T cells expressing IL-4 and IL-13 in tumor infiltrates and surrounding tissue (ST) were analyzed by flow cytometry. Dotted lines indicate paired samples from the same patient (n = 7, Wilcoxon matched-pairs ranked test). Single points indicate the percentage of cytokine expressing cells in tumor samples analyzed by flow cytometry for which we did not obtain sufficient number of cells from surrounding tissue to allow the analysis. (E) Frozen tissue sections from the same patient as in D were analyzed by immunofluorescence. Triple staining with anti-CD3-FITC (green), anti–IL-13–Texas red (red), and DAPI nuclear staining (blue). Bar, 90 µm.

Downloaded from jem.rupress.org on February 26, 2011

Published February 21, 2011

exposed to breast cancer supernatants. These were generated from established breast cancer cell lines expanded in vitro (Hs578T, MDA-MB-231, MDA-MB-468, MCF7, HCC-1806, and T47D; Table S2) and breast cancer tumors established in vivo by implanting breast cancer cell lines in immunodeficient mice (Aspord et al., 2007). As illustrated in Fig. 2 C, mDCs exposed for 48 h to Hs578T and HCC-1806 supernatants expressed OX40L. Four of the five breast cancer cell lines, with the notable exception of T47D, induced OX40L expression on mDCs (Fig. S1 C).

To test whether primary breast cancer tumors could also regulate OX40L expression, fragments of primary tumors were sonicated, centrifuged, filtered, and used in cultures with blood mDCs. As illustrated in Fig. 2 D, mDCs acquired both CD83 (a DC maturation marker) and OX40L. To determine the impact of OX40L on the generation of inflammatory Th2 responses in breast cancer, blood mDCs were first exposed for 48 h to either TSLP or breast tumor–soluble fractions. Exposed mDCs were then used to stimulate naive allogeneic CD4+ T cells with either the anti-OX40L antibody or a relevant

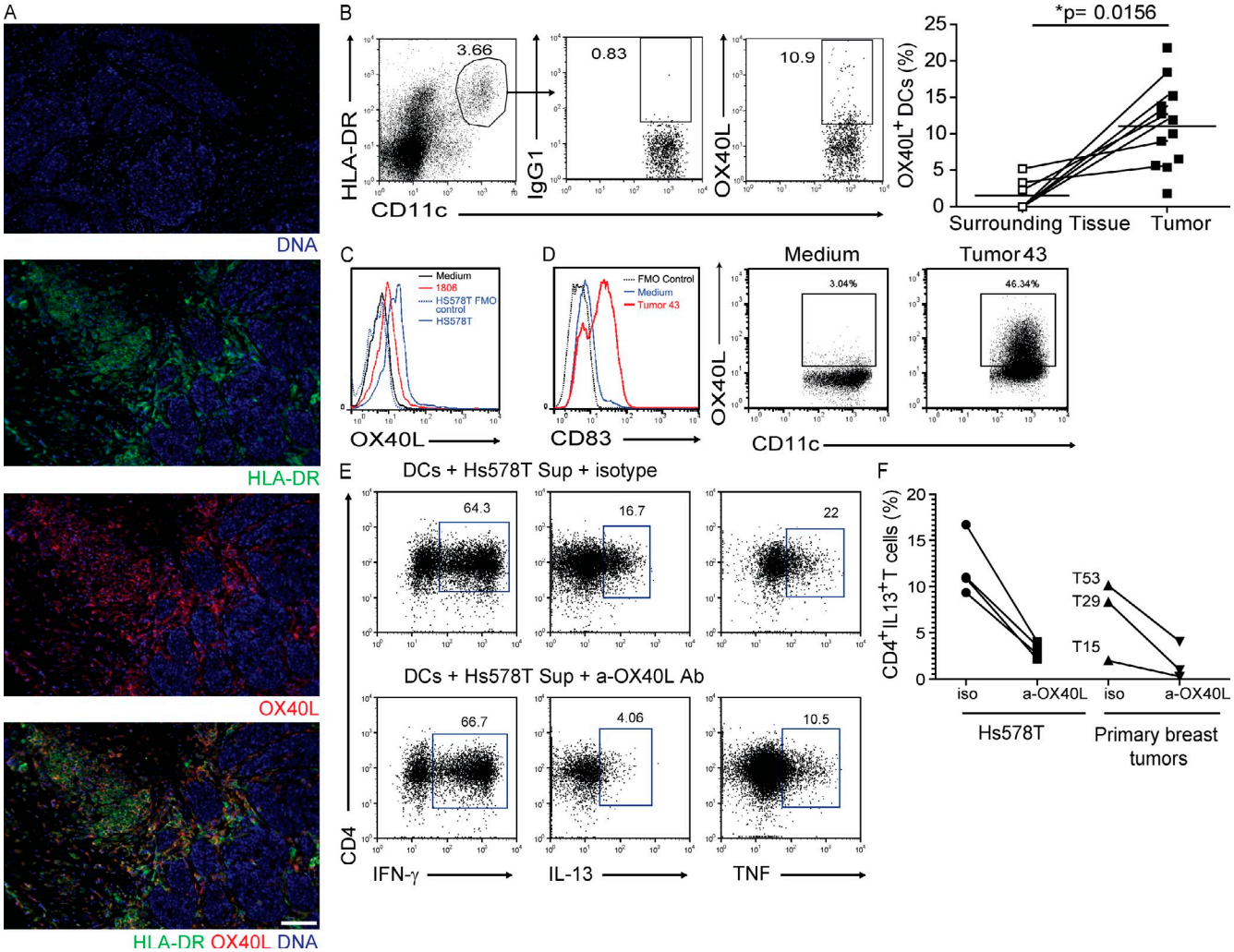

Figure 2. OX40L in breast cancer immune environment. (A) Immunofluorescence of primary breast tumor with indicated antibodies. Bar, 180 µm. Representative of 57/60 tumors analyzed. (B) Flow cytometry analysis of single-cell suspensions of primary breast tumors and surrounding tissue. Dot plots are gated on CD14^{neg} nonlymphocytes. OX40L expression is analyzed on HLA-DR^{high}CD11c^{high} DCs. Graph summarizes percentages of OX40L-expressing DCs in tumor infiltrates and surrounding tissue (ST) analyzed by flow cytometry. Dotted lines indicate paired samples from the same patient (Wilcoxon matched-pairs ranked test). Single points indicate the percentage of OX40L+ DCs in tumor samples for which we did not obtain sufficient number of cells from surrounding tissue to allow the analysis. (C and D) mDCs were exposed to media alone, to supernatant of breast cancer cell lines (1806 or Hs587T), or to sonicate of primary breast cancer tissue from patients (tumor 43). OX40L and CD83 were measured by flow cytometry. FMO, fluorescence minus one indicates controls where one staining fluorescence is omitted to set negative gate. (E and F) mDCs were exposed for 48 h to supernatants of breast cancer cells Hs578T, and then co-cultured with allogeneic naive CD4+ T cells in the presence of 40 µg/ml of anti-OX40L (Ik-5 clone) or isotype control antibody. After 1 wk, cells were collected and restimulated for 5 h with PMA/ionomycin for intracellular cytokine staining. Data in E are representative of four experiments. (F) Summary of the effect of blocking OX40L during T cell stimulation by tumor-activated DCs. Graph shows the proportion of IL-13–secreting cells induced by DCs activated with supernatants from breast cancer cell line Hs578T (left) or primary breast tumors (right, T15, T29, and T53).

Downloaded from jem.rupress.org on February 26, 2011

Published February 21, 2011

isotype control. Blocking OX40L prevented the expansion of IL13$^+$CD4$^+$ or TNF$^+$CD4$^+$ T cells by TSLP-primed mDCs (>50% inhibition; Fig. S2 A), mDCs exposed to Hs578T breast cancer cells (n = 4; median inhibition of IL13$^+$CD4$^+$ cells = 74%; range = 67–80%; Fig. 2, E and F), and mDCs exposed to sonicates of randomly selected primary breast cancer tumors (Fig. 2 F and Fig. S2 B). Thus, breast cancer cells produce factors that activate mDCs and induce them to express OX40L and to elicit inflammatory Th2 cells.

Breast cancer tumors express and secrete TSLP

OX40L can be induced on mDCs by TSLP, an IL-7–like cytokine produced by epithelial cells (Liu et al., 2007; Ziegler and Artis, 2010). All tested breast cancer cell lines expressed and secreted TSLP (Fig. 3 A). Supernatants of some primary breast cancer tumors stimulated with PMA and ionomycin displayed up to 300 pg/ml TSLP (Fig. 3 B). The expression of TSLP by cancer cells was further analyzed using an anti-TSLP antibody and immunofluorescence of frozen breast cancer tumors generated in the xenograft model (Aspord et al., 2007). There, subcutaneous MDA-MB-231 tumors transplanted in mice expressed TSLP (Fig. 3 C). The specificity of the staining is demonstrated by pretreatment of the antibody with recombinant TSLP (Fig. S3).

Importantly, TSLP is expressed in 35 out of 38 analyzed primary breast cancer tumors obtained from patients regardless of grade, histology, or stage of analyzed tumors. Fig. 3 D illustrates the pattern of TSLP staining and coexpression with

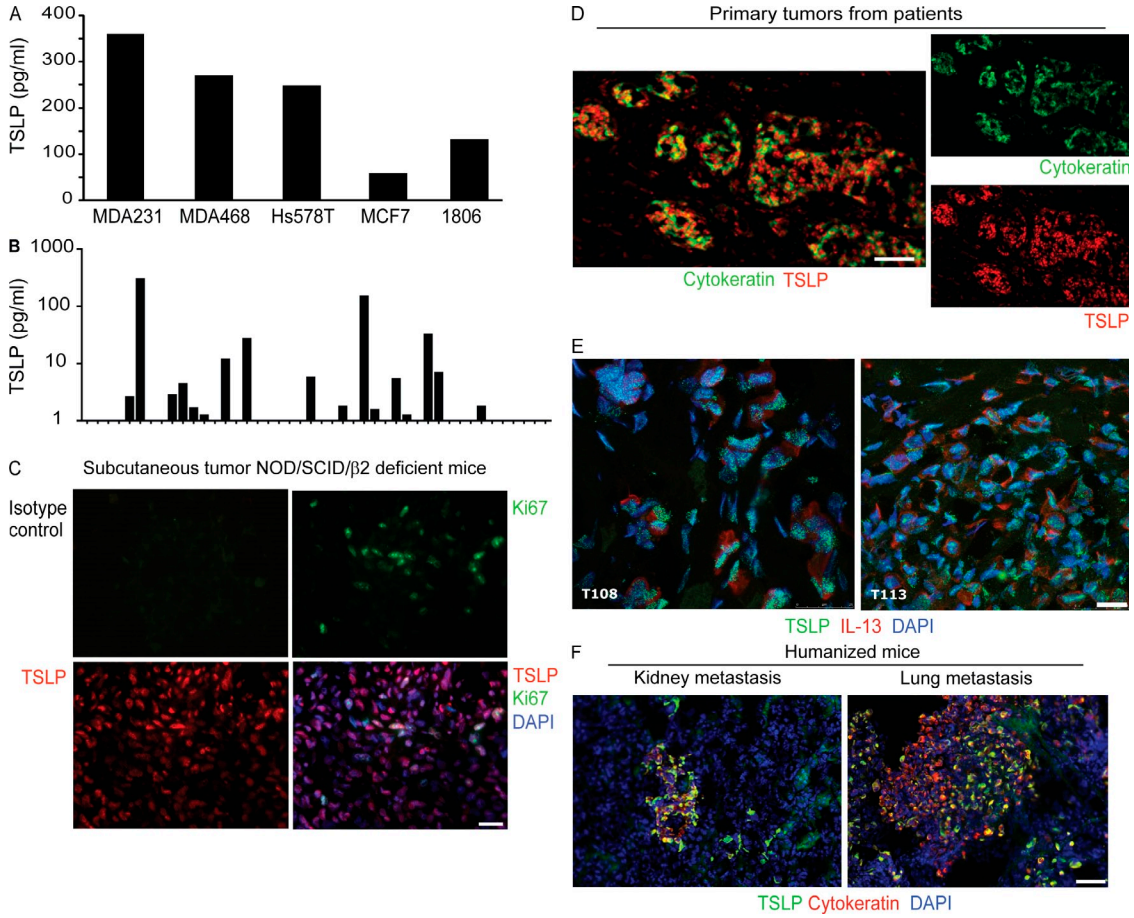

Figure 3. TSLP in breast cancer environment. (A) Luminex analysis of TSLP in supernatants of breast cancer cell lines after 24 h of culture in the presence of PMA and ionomycin. (B) Luminex analysis of TSLP levels in supernatants of primary breast tumors (from 44 patients) activated with PMA and ionomycin. (C) NOD/SCID/β2m$^{-/-}$ mice were irradiated the day before tumor implantation and 10 × 10^6 MDA-MB-231 cells were implanted by subcutaneous injection. Tumors were harvested at 4 wk after implant. Frozen tissue sections were analyzed by immunofluorescence for expression of TSLP (red). Actively dividing cells were identified by expression of Ki67 (green). Bar, 45 µm. (D and E) Frozen tissue sections from primary breast tumors from patients (38 patient samples) were analyzed by immunofluorescence for expression of TSLP. Tissues were also stained for the expression of IL-13 and cytokeratin 19, as indicated, to confirm TSLP expression by cancer cells. Staining pattern is representative of 35 out of 38 analyzed tumor samples from different patients. Bars: (D) 180 µm; (E) 15 µm. (F) NOD/SCID/β2m$^{-/-}$ mice were sublethally irradiated and transplanted with human CD34$^+$ HPCs by intravenous injection. 4 wk after HPC transplant, 5 × 10^6 MDA-MB-231 breast cancer cells were implanted subcutaneously. Tumors at the site of implantation, as well as lungs and kidneys, were harvested at 3 mo after implant. Frozen tissue sections were analyzed by immunofluorescence for expression of TSLP (green) and cytokeratin (red). Staining pattern is representative of tumors from three different mice. Bar, 90 µm.

Downloaded from jem.rupress.org on February 26, 2011

Published February 21, 2011

cytokeratin 19–positive cells. It demonstrates that TSLP is expressed in the cytoplasm and the nucleus of breast cancer cells that display IL-13 on their surface (Fig. 3 E). Importantly, TSLP is also expressed in lung and kidney metastasis of MDA-MB-231 tumors in humanized mice (Fig. 3 F) and in breast cancer tumor metastasis from patients (Fig. S4 A). TSLP expression is specific to epithelial cells as no staining can be found in tumor-infiltrating fibroblasts (Fig. S4 B). Furthermore, nonmalignant breast epithelia can also express TSLP (Fig. S4 C).

Thus, similar to normal skin or lung epithelium, breast epithelial cells and breast cancer cells have the capacity to express, produce, and secrete TSLP.

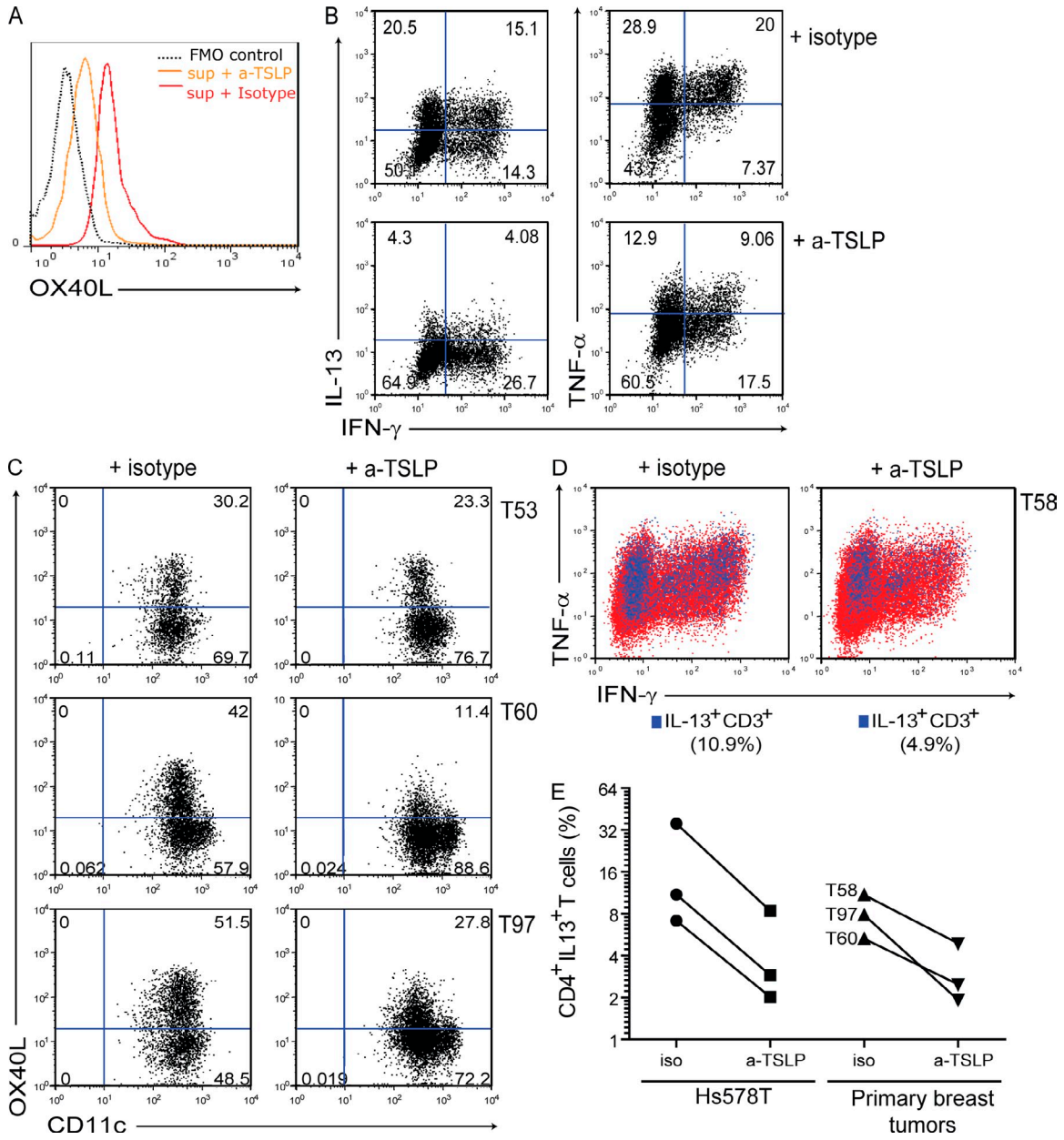

Figure 4. Blocking TSLP in vitro. (A) mDCs were incubated with supernatant of breast cancer cell line Hs578T in the presence or absence of 20 µg/ml of anti-TSLP (AB 19024; rabbit IgG). OX40L expression was measured by flow cytometry after 48 h of incubation. (B) mDCs treated as in A were co-cultured with naive allogeneic CD4+ T cells for 7 d. IL-13 production was measured by intracellular cytokine staining and flow cytometry after cells were restimulated for 5 h with PMA and ionomycin. Data are representative of three experiments. (C) mDCs were incubated with soluble factors from sonicated human breast tumors (T53, T60, and T97) in the presence or absence of 20 µg/ml of anti-TSLP (AB 19024; rabbit IgG). OX40L expression was measured by flow cytometry after 48 h of incubation. (D) mDCs treated as in C were co-cultured with naive allogeneic CD4+ T cells for 7 d. IL-13 production was measured by intracellular cytokine staining and flow cytometry after cells were restimulated for 5 h with PMA and ionomycin. Representative of three patients tested. Blue dots represent IL-13+ T cells gated in the same sample. (E) Graph shows data from three independent experiments as described in A–D.

Downloaded from jem.rupress.org on February 26, 2011

Published February 21, 2011

Anti-TSLP antibodies block the generation of inflammatory Th2 responses in vitro

To determine the impact of blocking TSLP on the generation of inflammatory Th2 responses in breast cancer, blood mDCs were first exposed for 48 h to either TSLP or breast tumor–soluble fractions. Addition of anti-TSLP–neutralizing antibodies to breast cancer tumor supernatants inhibited their ability to induce OX40L on mDCs (Fig. 4 A). Such mDCs displayed a diminished capacity to expand $IL13^+CD4^+$ or TNF^+CD4^+ T cells ($n = 3$; median inhibition = 73%, range = 72–77%; Fig. 4, B and E). Likewise, adding anti-TSLP–neutralizing antibody to sonicate of randomly selected primary breast cancer tumors led to down-regulation of OX40L expression by mDCs (Fig. 4 C) and decreased expansion of $IL13^+TNF^+CD4^+$ T cells (Fig. 4, D and E). Finally, when anti-TSLP receptor β chain (TSLPR) antibody was added to mDCs during their exposure to the supernatant of three different breast cancer cell lines (Hs578T, MDA-MB-231, and MCF7; Fig. 5 A), resulting mDCs showed a much diminished expansion of $IL13^+$ $CD4^+$ T cells (Fig. 5 B). Thus, TSLP is the factor secreted by breast cancer cells that contributes to generation of inflammatory Th2 responses.

Antibodies neutralizing TSLP–OX40L axis block tumor development in vivo

Our results thus far suggest a role for the TSLP–OX40L axis in generation of $IL13^+TNF^+CD4^+$ T cells, but do not establish whether this axis might actually contribute to breast cancer tumor development. To address this question, humanized mice were reconstituted with both Hs578T cells and T cells with or without anti-OX40L–, anti-TSLPR–, and anti-TSLP–neutralizing antibodies. As shown in Fig. 6 A, the administration of neutralizing anti-OX40L antibodies leads to significant inhibition of tumor development.

The administration of a neutralizing anti-TSLP antibody also results in the inhibition of tumor development (Fig. 6 B). TSLP blockade also leads to decreased secretion of IL-4 and IL-13 by tumor infiltrating T cells upon PMA and ionomycin activation (Fig. 6 C). Finally, the administration of antibody blocking TSLPR nearly completely blocks tumor development driven by $CD4^+$ T cells (Fig. 6 D). These results indicate that the TSLP contributes to breast cancer pathogenesis.

DISCUSSION

Here, we show that breast cancer is infiltrated with inflammatory Th2 cells and that such T cells are driven by OX40L on DCs. Blocking OX40L in vitro prevents generation of these $CD4^+$ T cells without impact on IL-10–producing $CD4^+$ T cells. Blocking OX40L in vivo partially prevents T cell–dependent acceleration of breast cancer tumor development. OX40L is not constitutively expressed, but can be induced on DCs, macrophages, and B cells; e.g., upon CD40 engagement or cytokine signals such as TSLP or IL-18, as well as upon TLR stimulation (Ito et al., 2005; Croft et al., 2009). Thus, the

Downloaded from jem.rupress.org on February 26, 2011

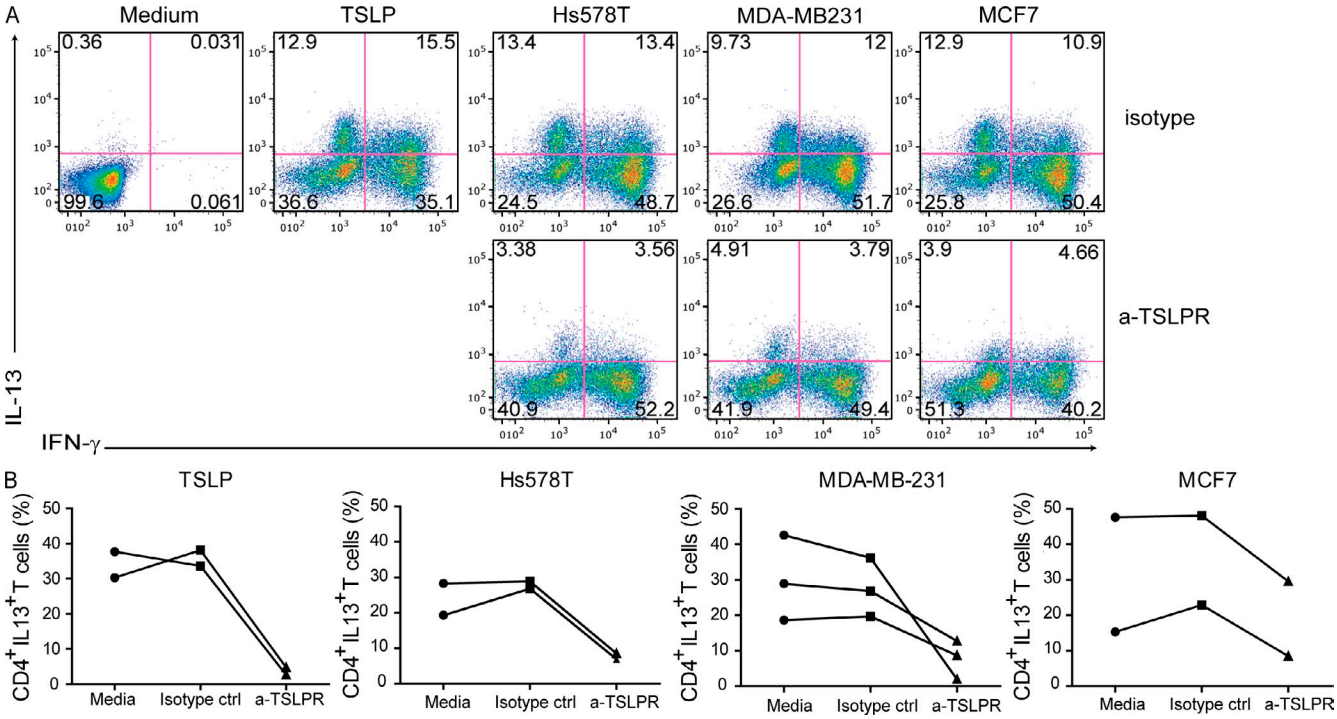

Figure 5. Blocking TSLP-R in vitro. (A) mDCs were treated with anti-TSLP-R (clone AB81_85.1F11, mouse IgG1), media or control antibody during activation with TSLP or with supernatant of one of the three different breast cancer cell lines (Hs578T, MDA-MB-231, and MCF7). mDCs were then co-cultured with allogeneic naive $CD4^+$ T cells. After 1 wk, cells were collected, restimulated for 5 h with PMA and ionomycin, and analyzed by flow cytometry. (B) Analysis of different experiments showing the effect of blocking TSLP-R on the induction of IL-13 secreting cells as described in A.

Published February 21, 2011

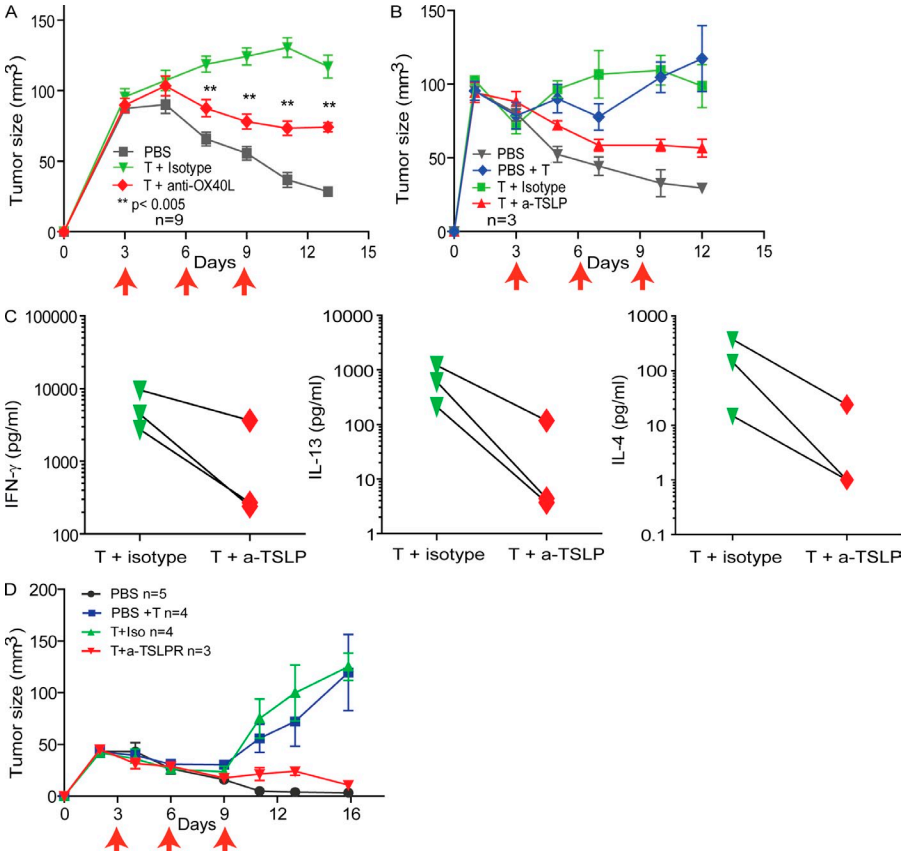

Figure 6. Blocking OX40L–TSLP in vivo. (A) NOD/SCID/β2m$^{-/-}$ mice were sublethally irradiated and transplanted with human CD34^{+} HPCs by intravenous injection. 4 wk after HPC transplant, 10 × 10^{6} Hs578T breast cancer cells were implanted subcutaneously. 3, 6, and 9 d after, mice were reconstituted with autologous total T cells together with 200 µg per injection of blocking anti-OX40L or isotype control antibody (mouse Ig; red arrows). PBS group was injected with tumor cells but not with T cells (gray line). Tumor size was measured at indicated times. Mean values from three experiments representing nine mice per each condition. Anti-OX40L and isotype-treated cohorts were compared statistically. (B) NOD/SCID/β2m$^{-/-}$ mice were irradiated and implanted with 10 × 10^{6} Hs578T breast cancer cells together with 200 µg per injection of neutralizing anti-TSLP (rabbit), rabbit isotype control antibody, or PBS. 3, 6, and 9 d after, mice were reconstituted with immature DCs and autologous total T cells together with 200 µg per injection of neutralizing anti-TSLP (rabbit), rabbit isotype control antibody or PBS. Representative of three independent experiments with a total of nine mice in TSLP blockade group. (C) Cytokine secretion in single-cell suspensions from tumors after 16-h restimulation with PMA and ionomycin. (D) Same as in B, but mice were injected with anti-TSLPR or isotype control at days 3, 6, and 9. Representative of two independent experiments. *n* indicates number of mice per cohort in this representative experiment.

presence of OX40L^{+} mDCs in breast tumors indicate sustained activation of DCs in tumor environment. Indeed, OX40L expression by DCs is driven by TSLP secreted from breast cancer cells. Accordingly, TSLP expression can be found in primary and metastatic tumors. Blocking TSLP reduces inflammation and partially inhibits tumor development.

Based on our results presented herein and in our earlier studies, we propose a vicious circle of smoldering type 2 inflammation that perpetuates breast cancer and which is maintained by TSLP. There, breast cancer attracts DCs, possibly through macrophage inflammatory protein 3 α (MIP3-α; Bell et al., 1999). Tumor-infiltrating DCs are then exposed to TSLP secreted by breast cancer cells, which triggers their maturation and OX40L expression. This might explain the aseptic mDC maturation that we found in breast cancer (Bell et al., 1999; Aspord et al., 2007). OX40L^{+} mDCs induce CD4^{+} T cells to secrete IL-13, as well as TNF. These inflammatory CD4^{+} T cells contribute to tumor development in an IL-13–dependent pathway (Aspord et al., 2007). Thus far, TSLP represents the only factor that activates mDCs without inducing them to produce Th1-polarizing cytokines (Liu et al., 2007). Under normal physiological conditions, TSLP appears to play a critical role in CD4^{+} T cell homeostasis in the peripheral mucosa-associated lymphoid tissues and in the positive selection and/or expansion of regulatory T (T reg) cells in the thymus (Watanabe et al., 2005a,b). In inflammatory conditions such as atopic dermatitis and asthma, epithelial cells markedly increase TSLP expression (Liu et al., 2007). The TSLP-activated DCs migrate to the draining lymph nodes, prime CD4^{+} T cells via OX40L to differentiate into inflammatory Th2 effector and memory cells, and thus initiate the adaptive phase of allergic immune responses. Interestingly, in breast cancer, OX40L^{+} mDCs are present in the tumor. It remains to be determined whether this reflects their inability to migrate from the tumor to draining lymph nodes. Indeed, such an evasion mechanism has been documented recently in human and mouse tumors showing an inhibition of DC migration from tumors to tumor-draining lymph nodes (Villablanca et al., 2010). This effect depends on tumor-derived ligands of the liver X receptors (Villablanca et al., 2010). It also remains to be determined whether these DCs are able to prime Th2 immunity in situ in tertiary lymphoid structures or whether their main role is to maintain the activation and survival of Th2 cells at the tumor site. Their ability to maintain Th2 cell phenotype and effector function is supported by our earlier studies showing that T cells isolated from experimental breast tumors and transferred to naive tumor-bearing humanized mice can promote tumor development even at low numbers and upon single injection (Aspord et al., 2007).

Downloaded from jem.rupress.org on February 26, 2011

Published February 21, 2011

Our results add another feature to the role of OX40L in tumors. Indeed, several studies in mouse models of transplantable tumors suggested that engaging OX40 via an agonist antibody, OX40L.Fc, or transfected tumor cells and DCs appears to promote antitumor effects (Weinberg et al., 2000; Morris et al., 2001; Ali et al., 2004; Piconese et al., 2008). However, *Tnfsf4* (gene coding OX40L) is regulated by the mRNA MIRN125B (Smirnov and Cheung, 2008), whose expression is down-regulated in breast cancer (Iorio et al., 2005). *Tnfsf4* is up-regulated in ataxia telangiectasia carriers and patients (Smirnov and Cheung, 2008), who have been shown to have an increased risk of breast cancer (Swift et al., 1987). Furthermore, a recent pilot study described the expression of OX40 and OX40L in >100 tissue samples from invasive ductal carcinomas, and suggested a possible association of OX40 expression and lymph node metastatic status (Xie et al., 2010). OX40L signaling has several important features that might help explain the results observed in our and other studies. Thus, OX40L triggers Th2 polarization independent of IL-4, promotes TNF production, and inhibits IL-10 production by the developing Th2 cells, but only in the absence of IL-12. In the presence of IL-12, OX40L signaling instead promotes the development of Th1 cells that, like inflammatory Th2 cells, produce TNF but not IL-10 (Liu et al., 2007).

Interestingly, inflammatory Th2 cells coexist within the tumor immune environment alongside IL-10–secreting $CD4^+$ T cells. Recent studies demonstrate a colocalization of cells with the phenotype of T reg cells) with mature DCs in lymphoid infiltrates in breast cancer (Gobert et al., 2009). A high number of $FoxP3^+$ T reg cells was associated with disease relapse (Gobert et al., 2009). Thus, the niche finding and metastasis formation might be facilitated by inflammatory Th2 response, whereas in the established tumor a T reg cell response might prevail. Interestingly, CCL22 (a macrophage-derived chemokine) appears involved in the attraction of T reg cells (Gobert et al., 2009), but also, in cooperation with CCL17 (TARC), of inflammatory Th2 cells (Liu et al., 2007). How this fine balance between T reg cells and Th2 responses is regulated will require further study.

Two key questions arise from our work: (1) what are the mechanisms allowing TSLP release from cancer cells; and (2) what is the impact of IL-13 (and IL-4) on cancer cells, on the stroma, and on the immune infiltrate? Our data show that nonmalignant breast epithelia can express TSLP. This further demonstrates that cancer cells can exploit pathways that are present in the normal tissue to establish a microenvironment facilitating tumor development. The mechanisms regulating TSLP expression and secretion from cancer cells, including a potential link with oncogenic events, remain to be established. It will also be important to determine the impact of TSLP and inflammatory Th2 environment on the stromal fibroblasts. Indeed, recent studies point to the critical role of cross talk between cancer cells and fibroblasts in determining the type of microenvironment established by cancer cells originating from different types of breast cancers (Camp et al., 2011).

Interestingly, studies in mice suggest the role of Th2 cytokines in mammary gland development. Indeed, the differentiation of the luminal epithelial lineage appears to require autocrine signaling by Th2 cytokines, as shown by reduced differentiation and alveolar morphogenesis in both Stat6 and IL-4–/IL-13–deficient mice during pregnancy (Khaled et al., 2007). Yet, in the murine model of endogenous breast cancer type 2, polarized $CD4^+$ T cells are essential to the metastatic process via secretion of IL-4, which induces macrophages to secrete epidermal growth factor (DeNardo et al., 2009). Similar to endogenous mouse model, in our model of transplanted metastatic human breast cancer IL-13 is derived from microenvironment. IL-13 can exert pro-cancer activity in several ways, including the triggering of TGF-β secretion (Terabe et al., 2000, 2003; Park et al., 2005; Shimamura et al., 2010). Furthermore, IL-4 exposure of cancer cells leads to the up-regulation of antiapoptotic pathways via mobilization of STAT6 (Zhang et al., 2008). We have shown that STAT6 is phosphorylated in primary breast cancer tumors (Aspord et al., 2007). All these antiapoptotic pathways are likely to synergize to promote the survival of cancer cells and facilitate metastasis. Importantly, such a protective effect on cancer cell susceptibility to apoptosis might increase their resistance to chemotherapy (Todaro et al., 2008) and immune-mediated cytotoxicity driven by Granzyme B (Sarin et al., 1997; Heibein et al., 2000). Thus, the TSLP–OX40L–IL13 axis might offer a novel therapeutic target.

MATERIALS AND METHODS

Isolation and culture of myeloid dendritic cells. DCs were purified from buffy coat of blood from healthy donors. In brief, DCs were enriched from mononuclear cells by negative selection using a mixture of antibodies against linage markers for CD3, CD14, CD16, CD19, CD56, and glycophorin A (Dynabeads Human DC Enrichment kit; Invitrogen). Cells from negative fraction were immunolabeled with anti–human FITC-labeled lienage cocktail (CD3, CD14, CD16, CD19, CD20, and CD56; BD); PE-labeled CD123 (mIgG1; clone 9F5; BD), QR-labeled HLA-DR (mIgG2a; clone HK14; Sigma-Aldrich) and APC-labeled CD11c (mIgG2b; clone S-HCL-3; BD). DCs (lin^-, $CD123^-$, $HLA\text{-}DR^+$, $CD11c^+$) were sorted in a FACSAria cytometer (BD). DCs were seeded at 100×10^3 cells/well in 200 µl of medium (RPMI supplemented with 2 mM glutamine, 50 U/ml penicillin, 50 µg/ml streptomycin, 0.1 mM MEM nonessential amino acids, 10 mM Hepes buffer, 0.1 mM sodium pyruvate, and 10% of human AB serum). DCs were cultured with medium alone or in the presence of 20 ng/ml of TSLP, or different tumor derived products. After 48 h, DCs were harvested and washed. The stimulated cells were stained for phenotype analysis or co-cultured with allogeneic naive $CD4^+$ T cells.

Immunofluorescence. 6-µm-frozen sections from tissues were fixed with cold acetone for 5 min. The sections were labeled with 5 µg/ml of anti-OX40L antibody (mouse IgG1, 8F4), followed by anti–mouse IgG conjugated to Texas red (Jackson ImmunoResearch Laboratories). For IL-13, tissue was labeled with 10 µg/ml of anti–IL-13 (polyclonal goat IgG; AF-123-NA; R&D System) followed with Texas red anti–goat IgG (Jackson ImmunoResearch Laboratories). TSLP was detected with 10 µg/ml of mouse anti-TSLP antibody prepared in-house (mIgG1; clone 14C3.2E11). Cytokeratin 19 was labeled with monoclonal antibody clone A53-BA2 (IgG2a; Abcam), followed by Alexa Fluor 568 goat anti–mouse IgG2a (Invitrogen). The following direct-labeled antibodies used were as follows: FITC anti–HLA-DR (mouse IgG2a; L243; BD), FITC anti-CD11c (clone; KB 90; Dako), FITC anti-Ki67

Downloaded from jem.rupress.org on February 26, 2011

(clone ki-67; Dako), and Alexa Fluor 488 anti-CD3 (mIgG1; UCHT1; BD). Finally, sections were counterstained for 2 min with 3 μM of the nuclear stain DAPI (in PBS; Invitrogen). To confirm specificity of TSLP staining, primary anti-TSLP antibody was preincubated with 100 μg of recombinant human TSLP (R&D Systems) for 30 min at room temperature before staining of tissue sections that previously showed to be TSLP positive.

Flow cytometry analysis. Cell suspensions from human breast carcinoma tissue and tumor or draining lymph nodes from humanized mice were used for phenotypic characterization of leukocytes. Cell suspensions were obtained by digestion with 2.5 mg/ml of collagenase D (Roche), and 200 U/ml of DNase I (Sigma-Aldrich) for 30–60 min at 37°C. The anti–human antibodies used were as follows: labeled FITC-labeled lineage cocktail (CD3, CD14, CD16, CD19, CD20, and CD56; BD); PE-labeled OX40L (mIgG1; clone Ik-1; BD); QR-labeled HLA-DR (mIgG2a; clone HK14; Sigma-Aldrich); APC-labeled CD11c (mIgG2b; clone S-HCL-3; BD); PerCP-labeled CD3 (mIgG1; clone SK7; BD); PECy7-labeled CD4 (mIgG1; clone SK3; BD); APCCy7-labeled CD8 (mIgG1; clone SK1; BD); CFS-labeled IL-4 (mIgG1; clone 3007; R&D Systems); Pacific blue–labeled IL-10 (rat IgG1; clone JES3-9D7; eBioscience); PE-labeled IL-13 (rat IgG1; clone JES10-5A2 BD); APC-labeled TNF (mIgG1; clone 6401.1111; BD); Alexa Fluor 700–labeled IFN-γ (mIgG1; clone B27; BD). Cells were incubated with the antibodies for 30 min at 4°C in the dark, and then washed three times and fixed with 1% paraformaldehyde to be analyzed in a FACSCalibur or LSR-II cytometer (BD). For intracellular cytokines, cells were stained using BD Cytofix/Cytoperm fixation/permeabilization kit according to the manufacturer's directions.

Tumor factors preparation. Tumor factors were obtained from supernatant of established breast cancer cell lines cultured in vitro (Table S2; Soule et al., 1973; Hackett et al., 1977; Lacroix and Leclercq, 2004; Neve et al., 2006) or by sonication from tumor cell lines, human breast tumor tissue, or tumors from humanized mice. In brief, cell lines were culture in medium (RPMI supplemented with 2 mM glutamine, 50 U/ml penicillin, 50 μg/ml streptomycin, 0.1 mM MEM nonessential amino acids, 10 mM Hepes buffer, 0.1 mM sodium pyruvate, and 10% fetal calf serum), and when the cells reached 90% of confluence fresh medium was added and the cells were left in culture for an additional 48 h. For sonication, cells or tissues were placed in PBS and disrupted for 30 s at 4°C, with the power output adjusted at 4.5 level of the 60 sonic dismembrator (Thermo Fisher Scientific). Cellular debris was removed by centrifugation, and the supernatant was collected and stored at −80°C.

Cytokine analysis. Tumor samples from patients diagnosed with breast carcinoma (in situ, invasive duct, and/or mucinous carcinoma of the breast, as well as lobular carcinoma) were obtained from the Baylor University Medical Center Tissue Bank (Institutional Review Board no. 005–145). Tumors and draining lymph nodes from mice implanted with breast cancer cell lines H578T and MDA-MB-231 were also analyzed. Whole-tissue fragments (4 × 4 × 4 mm, 0.02 g, approximately) were placed in culture medium with 50 ng/ml of PMA (Sigma-Aldrich) and 1 μg/ml of ionomycin (Sigma-Aldrich) for 16 h. Cytokine production was analyzed in the culture supernatant by Luminex. For intracellular staining, cells were resuspended at a concentration of 10^6 cells/ml in medium and activated for 5 h with PMA and ionomycin; brefeldin A (GolgiPlug; BD) and monensin (GolgiStop; BD) were added for the last 2.5 h.

DC–T cell co-cultures. Total $CD4^+$ T cells were enriched from PBMCs of healthy donors using magnetic depletion of other leukocytes (EasySep Human $CD4^+$ T Cell Enrichment kit; STEMCELL Technologies, Inc.). Naive $CD4^+$ T cells were sorted based on the expression of $CD4^+$ $CD27^+$ and $CD45RA^+$. Activated mDCs with medium, TSLP, or tumor-derived factors were co-cultured with naive $CD4^+$ T cells at a ratio of 1:5 for 7 d. After that, the cells were washed and restimulated for 5 h with 50 ng/ml PMA and 1 μl/ml ionomycin. Brefeldin A and monensin were added for the last 2.5 h, followed by surface and intracellular staining. For blocking OX40L, tumor-activated mDCs were co-cultured with naive CD4 T cells in the presence of 50 μg of anti-OX40L (Ik-5 clone) or control IgG2a isotype antibody. For blocking TSLP, tumor-derived factors were preincubated with 20 μg/ml of anti-TSLP antibody (rabbit; AB 19024) or normal rabbit IgG (R&D Systems) at room temperature for 30 min after DC activation. DCs were activated with the neutralized tumor-derived factors and finally co-cultured with naive CD4 T cells for 7 d. For TSLPR blocking, DCs were preincubated with anti-TSLP receptor antibody (clone AB81_85.1F11; mouse IgG1) for 3 min at room temperature.

Tumor-bearing mice. Mice were humanized either by $CD34^+$ hematopoietic progenitor cell (HPC) transplant or by co-administration of DCs and T cells as described previously (Aspord et al., 2007; Institutional Animal Care and Use Committee no. A01-005). $CD34^+$HPCs were obtained from apheresis of adult healthy volunteers mobilized with G-CSF and purified as described previously (Aspord et al., 2007). The $CD34^-$ fraction of apheresis was Ficoll purified, and the PBMCs obtained were stored frozen and used as a source of autologous T cells. 3 million $CD34^+$ HPCs were transplanted intravenously into sublethally irradiated (12 cGy/g body weight of 137Cs γ irradiation) nonobese diabetic/LtSz-scid/scid β2 microglobulin–deficient (NOD/SCID/$\beta 2m^{-/-}$) mice (Jackson ImmunoResearch Laboratories). After 4 wk of engraftment, 10 million Hs578T breast cancer cells were harvested from cultures and injected subcutaneously into the flanks of the mice. Mice were reconstituted with 10 million $CD4^+$ T cells and 10 million $CD8^+$ T cells autologous to the grafted $CD34^+$ HPCs. $CD4^+$ and $CD8^+$ T cells were positively selected from thawed PBMCs using magnetic selection according to the manufacturer's instructions (Miltenyi Biotec). The purity was routinely >90%. T cells were transferred at days 3, 6, and 9 after tumor implantation. For experiments with NOD/SCID/$\beta 2m^{-/-}$ mice, they were sublethally irradiated the day before tumor implantation. Mice were then reconstituted with 1 million monocyte-derived DCs (MDDCs) and autologous T cells as described in the previous paragraph. MDDCs were generated from the adherent fraction of PBMCs by culturing with 100 ng/ml GM-CSF (Immunex) and 10 ng/ml IL-4 (R&D Systems). Tumor size was monitored every 2–3 d. Tumor volume (ellipsoid) was calculated as follows: ([short diameter]^2 × long diameter)/2.

Blocking in vivo experiments. For different experimental purposes, tumor-bearing mice transferred with autologous T cells were injected intratumorally with 200 μg of anti-OX40L (clone IK-5; mIgG2a) blocking antibody, 100 μg of anti-TSLP antibody (clone AB19024; rabbit IgG), 100 μg of anti-IL-13 neutralizing antibody prepared in-house (clone 13G1.B2; mIgG1), 200 μg of anti-TSLPR neutralizing antibody (clone AB81_85.1F11; mouse IgG1), or isotype control, respectively at days 3, 6, and 9 after tumor implantation. For blocking TSLP, anti-TSLP antibody injection was also given at day 0 while the tumor was implanted.

Online supplemental material. Fig. S1 illustrates gating strategy for flow cytometry analysis of tumor-infiltrating lymphocytes and the accumulation of lymphocytes in tumor beds as compared with surrounding tissue. Fig. S2 shows that mDCs exposed to TSLP or to soluble tumor factors in the presence of anti-OX40L are unable to drive the differentiation of inflammatory Th2 cells. Fig. S3 shows the specificity of anti-TSLP antibody staining in frozen tissue sections. Fig. S4 shows the expression of TSLP in breast cancer cells and in nonmalignant breast tissue. Table S1 provides the pathological diagnosis information and Luminex data for cytokine levels of all 99 breast cancer patients used for cytokine analysis. Table S2 describes the characteristics of breast cancer cell lines studied. Online supplemental material is available at http://www.jem.org/cgi/content/full/jem.20102131/DC1.

We are grateful to Albert Barnes, Sebastien Coquery, Elizabeth Kraus, Mark Michnevitz, Gina Stella Garcia-Romo, Jenny Smith, and Lynnette Walters for help; Dr. Joseph Fay for help with healthy volunteers; Cindy Samuelsen for continuous support; and Drs. Sally M. Knox and Michael Grant at the Department of Surgery

Downloaded from jem.rupress.org on February 26, 2011

Published February 21, 2011

and Ms. Dan Su at the Department of Pathology at Baylor University Medical Center. We thank Dr. Michael Ramsay for continuous support.

This work was supported by the Baylor Health Care Systems Foundation, and the National Institutes of Health (grants R0-1 CA89440 and R21 AI056001 to A. Karolina Palucka; grants U19 AI057234, R0-1 CA78846, and CA85540 to J. Banchereau).

J. Banchereau holds the Caruth Chair for Transplantation Immunology Research.

A. Karolina Palucka holds the Ramsay Chair for Cancer Immunology Research.

The authors have no conflicting financial interests.

Submitted: 7 October 2010
Accepted: 27 January 2011

REFERENCES

Ali, S.A., M. Ahmad, J. Lynam, C.S. McLean, C. Entwisle, P. Loudon, E. Choolun, S.E. McArdle, G. Li, S. Mian, and R.C. Rees. 2004. Antitumour therapeutic efficacy of OX40L in murine tumour model. *Vaccine*. 22:3585–3594. doi:10.1016/j.vaccine.2004.03.041

Aspord, C., A. Pedroza-Gonzalez, M. Gallegos, S. Tindle, E.C. Burton, D. Su, F. Marches, J. Banchereau, and A.K. Palucka. 2007. Breast cancer instructs dendritic cells to prime interleukin 13–secreting CD4+ T cells that facilitate tumor development. *J. Exp. Med*. 204:1037–1047. doi:10.1084/jem.20061120

Bell, D., P. Chomarat, D. Broyles, G. Netto, G.M. Harb, S. Lebecque, J. Valladeau, J. Davoust, K.A. Palucka, and J. Banchereau. 1999. In breast carcinoma tissue, immature dendritic cells reside within the tumor, whereas mature dendritic cells are located in peritumoral areas. *J. Exp. Med*. 190:1417–1426. doi:10.1084/jem.190.10.1417

Berzofsky, J.A., and M. Terabe. 2008. A novel immunoregulatory axis of NKT cell subsets regulating tumor immunity. *Cancer Immunol. Immunother.* 57:1679–1683. doi:10.1007/s00262-008-0495-4

Brimnes, M.K., L. Bonifaz, R.M. Steinman, and T.M. Moran. 2003. Influenza virus–induced dendritic cell maturation is associated with the induction of strong T cell immunity to a coadministered, normally nonimmunogenic protein. *J. Exp. Med*. 198:133–144. doi:10.1084/jem.20030266

Camp, J.T., F. Elloumi, E. Roman-Perez, J. Rein, D.A. Stewart, J.C. Harrell, C.M. Perou, and M.A. Troester. 2011. Interactions with fibroblasts are distinct in Basal-like and luminal breast cancers. *Mol. Cancer Res.* 9:3–13. doi:10.1158/1541-7786.MCR-10-0372

Caux, C., C. Massacrier, B. Vanbervliet, B. Dubois, I. Durand, M. Cella, A. Lanzavecchia, and J. Banchereau. 1997. CD34+ hematopoietic progenitors from human cord blood differentiate along two independent dendritic cell pathways in response to granulocyte-macrophage colony-stimulating factor plus tumor necrosis factor alpha: II. Functional analysis. *Blood*. 90:1458–1470.

Condeelis, J., and J.W. Pollard. 2006. Macrophages: obligate partners for tumor cell migration, invasion, and metastasis. *Cell*. 124:263–266. doi:10.1016/j.cell.2006.01.007

Coughlin, S.S., and D.U. Ekwueme. 2009. Breast cancer as a global health concern. *Cancer Epidemiol*. 33:315–318. doi:10.1016/j.canep.2009.10.003

Coussens, L.M., and Z. Werb. 2002. Inflammation and cancer. *Nature*. 420:860–867. doi:10.1038/nature01322

Croft, M., T. So, W. Duan, and P. Soroosh. 2009. The significance of OX40 and OX40L to T-cell biology and immune disease. *Immunol. Rev.* 229:173–191. doi:10.1111/j.1600-065X.2009.00766.x

DeNardo, D.G., J.B. Barreto, P. Andreu, L. Vasquez, D. Tawfik, N. Kolhatkar, and L.M. Coussens. 2009. CD4(+) T cells regulate pulmonary metastasis of mammary carcinomas by enhancing protumor properties of macrophages. *Cancer Cell*. 16:91–102. doi:10.1016/j.ccr.2009.06.018

Dudziak, D., A.O. Kamphorst, G.F. Heidkamp, V.R. Buchholz, C. Trumpfheller, S. Yamazaki, C. Cheong, K. Liu, H.W. Lee, C.G. Park, et al. 2007. Differential antigen processing by dendritic cell subsets *in vivo*. *Science*. 315:107–111. doi:10.1126/science.1136080

Finkelman, F.D., A. Lees, R. Birnbaum, W.C. Gause, and S.C. Morris. 1996. Dendritic cells can present antigen in vivo in a tolerogenic or immunogenic fashion. *J. Immunol.* 157:1406–1414.

Gilliet, M., V. Soumelis, N. Watanabe, S. Hanabuchi, S. Antonenko, R. de Waal-Malefyt, and Y.J. Liu. 2003. Human dendritic cells activated by TSLP and CD40L induce proallergic cytotoxic T cells. *J. Exp. Med*. 197:1059–1063. doi:10.1084/jem.20030240

Gobert, M., I. Treilleux, N. Bendriss-Vermare, T. Bachelot, S. Goddard-Leon, V. Arfi, C. Biota, A.C. Doffin, I. Durand, D. Olive, et al. 2009. Regulatory T cells recruited through CCL22/CCR4 are selectively activated in lymphoid infiltrates surrounding primary breast tumors and lead to an adverse clinical outcome. *Cancer Res.* 69:2000–2009. doi:10.1158/0008-5472.CAN-08-2360

Grivennikov, S.I., F.R. Greten, and M. Karin. 2010. Immunity, inflammation, and cancer. *Cell*. 140:883–899. doi:10.1016/j.cell.2010.01.025

Hackett, A.J., H.S. Smith, E.L. Springer, R.B. Owens, W.A. Nelson-Rees, J.L. Riggs, and M.B. Gardner. 1977. Two syngeneic cell lines from human breast tissue: the aneuploid mammary epithelial (Hs578T) and the diploid myoepithelial (Hs578Bst) cell lines. *J. Natl. Cancer Inst*. 58:1795–1806.

Hawiger, D., K. Inaba, Y. Dorsett, M. Guo, K. Mahnke, M. Rivera, J.V. Ravetch, R.M. Steinman, and M.C. Nussenzweig. 2001. Dendritic cells induce peripheral T cell unresponsiveness under steady state conditions in vivo. *J. Exp. Med*. 194:769–779. doi:10.1084/jem.194.6.769

Heibein, J.A., I.S. Goping, M. Barry, M.J. Pinkoski, G.C. Shore, D.R. Green, and R.C. Bleackley. 2000. Granzyme B-mediated cytochrome c release is regulated by the Bcl-2 family members bid and Bax. *J. Exp. Med*. 192:1391–1402. doi:10.1084/jem.192.10.1391

Iorio, M.V., M. Ferracin, C.G. Liu, A. Veronese, R. Spizzo, S. Sabbioni, E. Magri, M. Pedriali, M. Fabbri, M. Campiglio, et al. 2005. MicroRNA gene expression deregulation in human breast cancer. *Cancer Res.* 65:7065–7070. doi:10.1158/0008-5472.CAN-05-1783

Ito, T., Y.H. Wang, O. Duramad, T. Hori, G.J. Delespesse, N. Watanabe, F.X. Qin, Z. Yao, W. Cao, and Y.J. Liu. 2005. TSLP-activated dendritic cells induce an inflammatory T helper type 2 cell response through OX40 ligand. *J. Exp. Med*. 202:1213–1223. doi:10.1084/jem.20051135

Kapp, U., W.C. Yeh, B. Patterson, A.J. Elia, D. Kägi, A. Ho, A. Hessel, M. Tipsword, A. Williams, C. Mirtsos, et al. 1999. Interleukin 13 is secreted by and stimulates the growth of Hodgkin and Reed-Sternberg cells. *J. Exp. Med*. 189:1939–1946. doi:10.1084/jem.189.12.1939

Khaled, W.T., E.K. Read, S.E. Nicholson, F.O. Baxter, A.J. Brennan, P.J. Came, N. Sprigg, A.N. McKenzie, and C.J. Watson. 2007. The IL-4/IL-13/Stat6 signalling pathway promotes luminal mammary epithelial cell development. *Development*. 134:2739–2750. doi:10.1242/dev.003194

Klechevsky, E., R. Morita, M. Liu, Y. Cao, S. Coquery, L. Thompson-Snipes, F. Briere, D. Chaussabel, G. Zurawski, A.K. Palucka, et al. 2008. Functional specializations of human epidermal Langerhans cells and CD14+ dermal dendritic cells. *Immunity*. 29:497–510. doi:10.1016/j.immuni.2008.07.013

Lacroix, M., and G. Leclercq. 2004. Relevance of breast cancer cell lines as models for breast tumours: an update. *Breast Cancer Res. Treat*. 83:249–289. doi:10.1023/B:BREA.0000014042.54925.cc

Levings, M.K., S. Gregori, E. Tresoldi, S. Cazzaniga, C. Bonini, and M.G. Roncarolo. 2005. Differentiation of Tr1 cells by immature dendritic cells requires IL-10 but not CD25+CD4+ Tr cells. *Blood*. 105:1162–1169. doi:10.1182/blood-2004-03-1211

Liu, Y.J., V. Soumelis, N. Watanabe, T. Ito, Y.H. Wang, R.de.W. Malefyt, M. Omori, B. Zhou, and S.F. Ziegler. 2007a. TSLP: an epithelial cell cytokine that regulates T cell differentiation by conditioning dendritic cell maturation. *Annu. Rev. Immunol*. 25:193–219. doi:10.1146/annurev.immunol.25.022106.141718

Luft, T., M. Jefford, P. Luetjens, T. Toy, H. Hochrein, K.A. Masterman, C. Maliszewski, K. Shortman, J. Cebon, and E. Maraskovsky. 2002. Functionally distinct dendritic cell (DC) populations induced by physiologic stimuli: prostaglandin E(2) regulates the migratory capacity of specific DC subsets. *Blood*. 100:1362–1372. doi:10.1182/blood-2001-12-0360

Maldonado-López, R., T. De Smedt, P. Michel, J. Godfroid, B. Pajak, C. Heirman, K. Thielemans, O. Leo, J. Urbain, and M. Moser. 1999. CD8alpha+ and CD8alpha- subclasses of dendritic cells direct the development of distinct T helper cells in vivo. *J. Exp. Med*. 189:587–592. doi:10.1084/jem.189.3.587

Mantovani, A., and A. Sica. 2010. Macrophages, innate immunity and cancer: balance, tolerance, and diversity. *Curr. Opin. Immunol*. 22:231–237. doi:10.1016/j.coi.2010.01.009

Downloaded from jem.rupress.org on February 26, 2011

Mantovani, A., P. Romero, A.K. Palucka, and F.M. Marincola. 2008. Tumour immunity: effector response to tumour and role of the microenvironment. *Lancet*. 371:771–783. doi:10.1016/S0140-6736(08)60241-X

Morris, A., J.T. Vetto, T. Ramstad, C.J. Funatake, E. Choolun, C. Entwisle, and A.D. Weinberg. 2001. Induction of anti-mammary cancer immunity by engaging the OX-40 receptor in vivo. *Breast Cancer Res. Treat*. 67:71–80. doi:10.1023/A:1010649303056

Neve, R.M., K. Chin, J. Fridlyand, J. Yeh, F.L. Baehner, T. Fevr, L. Clark, N. Bayani, J.P. Coppe, F. Tong, et al. 2006. A collection of breast cancer cell lines for the study of functionally distinct cancer subtypes. *Cancer Cell*. 10:515–527. doi:10.1016/j.ccr.2006.10.008

Park, J.M., M. Terabe, L.T. van den Broeke, D.D. Donaldson, and J.A. Berzofsky. 2005. Unmasking immunosurveillance against a syngeneic colon cancer by elimination of CD4+ NKT regulatory cells and IL-13. *Int. J. Cancer*. 114:80–87. doi:10.1002/ijc.20669

Park, J.M., M. Terabe, D.D. Donaldson, G. Forni, and J.A. Berzofsky. 2008. Natural immunosurveillance against spontaneous, autochthonous breast cancers revealed and enhanced by blockade of IL-13-mediated negative regulation. *Cancer Immunol. Immunother.* 57:907–912. doi:10.1007/s00262-007-0414-0

Piconese, S., B. Valzasina, and M.P. Colombo. 2008. OX40 triggering blocks suppression by regulatory T cells and facilitates tumor rejection. *J. Exp. Med*. 205:825–839. doi:10.1084/jem.20071341

Pulendran, B., J.L. Smith, G. Caspary, K. Brasel, D. Pettit, E. Maraskovsky, and C.R. Maliszewski. 1999. Distinct dendritic cell subsets differentially regulate the class of immune response in vivo. *Proc. Natl. Acad. Sci. USA*. 96:1036–1041. doi:10.1073/pnas.96.3.1036

Rakoff-Nahoum, S., and R. Medzhitov. 2009. Toll-like receptors and cancer. *Nat. Rev. Cancer*. 9:57–63. doi:10.1038/nrc2541

Sarin, A., M.S. Williams, M.A. Alexander-Miller, J.A. Berzofsky, C.M. Zacharchuk, and P.A. Henkart. 1997. Target cell lysis by CTL granule exocytosis is independent of ICE/Ced-3 family proteases. *Immunity*. 6:209–215. doi:10.1016/S1074-7613(00)80427-6

Shimamura, T., T. Fujisawa, S.R. Husain, B. Joshi, and R.K. Puri. 2010. Interleukin 13 mediates signal transduction through interleukin 13 receptor alpha2 in pancreatic ductal adenocarcinoma: role of IL-13 Pseudomonas exotoxin in pancreatic cancer therapy. *Clin. Cancer Res.* 16:577–586. doi:10.1158/1078-0432.CCR-09-2015

Skinnider, B.F., A.J. Elia, R.D. Gascoyne, L.H. Trümper, F. von Bonin, U. Kapp, B. Patterson, B.E. Snow, and T.W. Mak. 2001. Interleukin 13 and interleukin 13 receptor are frequently expressed by Hodgkin and Reed-Sternberg cells of Hodgkin lymphoma. *Blood*. 97:250–255. doi:10.1182/blood.V97.1.250

Skinnider, B.F., A.J. Elia, R.D. Gascoyne, B. Patterson, L. Trumper, U. Kapp, and T.W. Mak. 2002. Signal transducer and activator of transcription 6 is frequently activated in Hodgkin and Reed-Sternberg cells of Hodgkin lymphoma. *Blood*. 99:618–626. doi:10.1182/blood.V99.2.618

Smirnov, D.A., and V.G. Cheung. 2008. ATM gene mutations result in both recessive and dominant expression phenotypes of genes and microRNAs. *Am. J. Hum. Genet*. 83:243–253. doi:10.1016/j.ajhg.2008.07.003

Soule, H.D., J. Vazguez, A. Long, S. Albert, and M. Brennan. 1973. A human cell line from a pleural effusion derived from a breast carcinoma. *J. Natl. Cancer Inst*. 51:1409–1416.

Soumelis, V., P.A. Reche, H. Kanzler, W. Yuan, G. Edward, B. Homey, M. Gilliet, S. Ho, S. Antonenko, A. Lauerma, et al. 2002. Human epithelial cells trigger dendritic cell mediated allergic inflammation by producing TSLP. *Nat. Immunol.* 3:673–680.

Steinbrink, K., H. Jonuleit, G. Müller, G. Schuler, J. Knop, and A.H. Enk. 1999. Interleukin-10-treated human dendritic cells induce a melanoma-antigen-specific anergy in CD8(+) T cells resulting in a failure to lyse tumor cells. *Blood*. 93:1634–1642.

Steinman, R.M., and J. Banchereau. 2007. Taking dendritic cells into medicine. *Nature*. 449:419–426. doi:10.1038/nature06175

Steinman, R.M., D. Hawiger, and M.C. Nussenzweig. 2003. Tolerogenic dendritic cells. *Annu. Rev. Immunol*. 21:685–711. doi:10.1146/annurev.immunol.21.120601.141040

Swift, M., P.J. Reitnauer, D. Morrell, and C.L. Chase. 1987. Breast and other cancers in families with ataxia-telangiectasia. *N. Engl. J. Med*. 316:1289–1294. doi:10.1056/NEJM198705213162101

Terabe, M., S. Matsui, N. Noben-Trauth, H. Chen, C. Watson, D.D. Donaldson, D.P. Carbone, W.E. Paul, and J.A. Berzofsky. 2000. NKT cell-mediated repression of tumor immunosurveillance by IL-13 and the IL-4R-STAT6 pathway. *Nat. Immunol.* 1:515–520. doi:10.1038/82771

Terabe, M., S. Matsui, J.M. Park, M. Mamura, N. Noben-Trauth, D.D. Donaldson, W. Chen, S.M. Wahl, S. Ledbetter, B. Pratt, et al. 2003. Transforming growth factor-beta production and myeloid cells are an effector mechanism through which CD1d-restricted T cells block cytotoxic T lymphocyte-mediated tumor immunosurveillance: abrogation prevents tumor recurrence. *J. Exp. Med*. 198:1741–1752. doi:10.1084/jem.20022227

Todaro, M., Y. Lombardo, M.G. Francipane, M.P. Alea, P. Cammareri, F. Iovino, A.B. Di Stefano, C. Di Bernardo, A. Agrusa, G. Condorelli, et al. 2008. Apoptosis resistance in epithelial tumors is mediated by tumor-cell-derived interleukin-4. *Cell Death Differ.* 15:762–772. doi:10.1038/sj.cdd.4402305

Trieu, Y., X.Y. Wen, B.F. Skinnider, M.R. Bray, Z. Li, J.O. Claudio, E. Masih-Khan, Y.X. Zhu, S. Trudel, J.A. McCart, et al. 2004. Soluble interleukin-13Ralpha2 decoy receptor inhibits Hodgkin's lymphoma growth in vitro and in vivo. *Cancer Res.* 64:3271–3275. doi:10.1158/0008-5472.CAN-03-3764

Villablanca, E.J., L. Raccosta, D. Zhou, R. Fontana, D. Maggioni, A. Negro, F. Sanvito, M. Ponzoni, B. Valentinis, M. Bregni, et al. 2010. Tumor-mediated liver X receptor-alpha activation inhibits CC chemokine receptor-7 expression on dendritic cells and dampens antitumor responses. *Nat. Med*. 16:98–105. doi:10.1038/nm.2074

Watanabe, N., S. Hanabuchi, M.A. Marloie-Provost, S. Antonenko, Y.J. Liu, and V. Soumelis. 2005a. Human TSLP promotes CD40 ligand-induced IL-12 production by myeloid dendritic cells but maintains their Th2 priming potential. *Blood*. 105:4749–4751. doi:10.1182/blood-2004-09-3622

Watanabe, N., Y.H. Wang, H.K. Lee, T. Ito, Y.H. Wang, W. Cao, and Y.J. Liu. 2005b. Hassall's corpuscles instruct dendritic cells to induce CD4+CD25+ regulatory T cells in human thymus. *Nature*. 436:1181–1185. doi:10.1038/nature03886

Weinberg, A.D., M.M. Rivera, R. Prell, A. Morris, T. Ramstad, J.T. Vetto, W.J. Urba, G. Alvord, C. Bunce, and J. Shields. 2000. Engagement of the OX-40 receptor in vivo enhances antitumor immunity. *J. Immunol*. 164:2160–2169.

Xie, F., Q. Wang, Y. Chen, Y. Gu, H. Mao, W. Zeng, and X. Zhang. 2010. Costimulatory molecule OX40/OX40L expression in ductal carcinoma in situ and invasive ductal carcinoma of breast: an immunohistochemistry-based pilot study. *Pathol. Res. Pract*. 206:735–739. doi:10.1016/j.prp.2010.05.016

Zhang, W.J., B.H. Li, X.Z. Yang, P.D. Li, Q. Yuan, X.H. Liu, S.B. Xu, Y. Zhang, J. Yuan, G.S. Gerhard, et al. 2008. IL-4-induced Stat6 activities affect apoptosis and gene expression in breast cancer cells. *Cytokine*. 42:39–47. doi:10.1016/j.cyto.2008.01.016

Ziegler, S.F., and D. Artis. 2010. Sensing the outside world: TSLP regulates barrier immunity. *Nat. Immunol*. 11:289–293. doi:10.1038/ni.1852

Downloaded from jem.rupress.org on February 26, 2011

The Journal of Experimental Medicine

SUPPLEMENTAL MATERIAL

Pedroza-Gonzalez et al., http://www.jem.org/cgi/content/full/jem.20102131/DC1

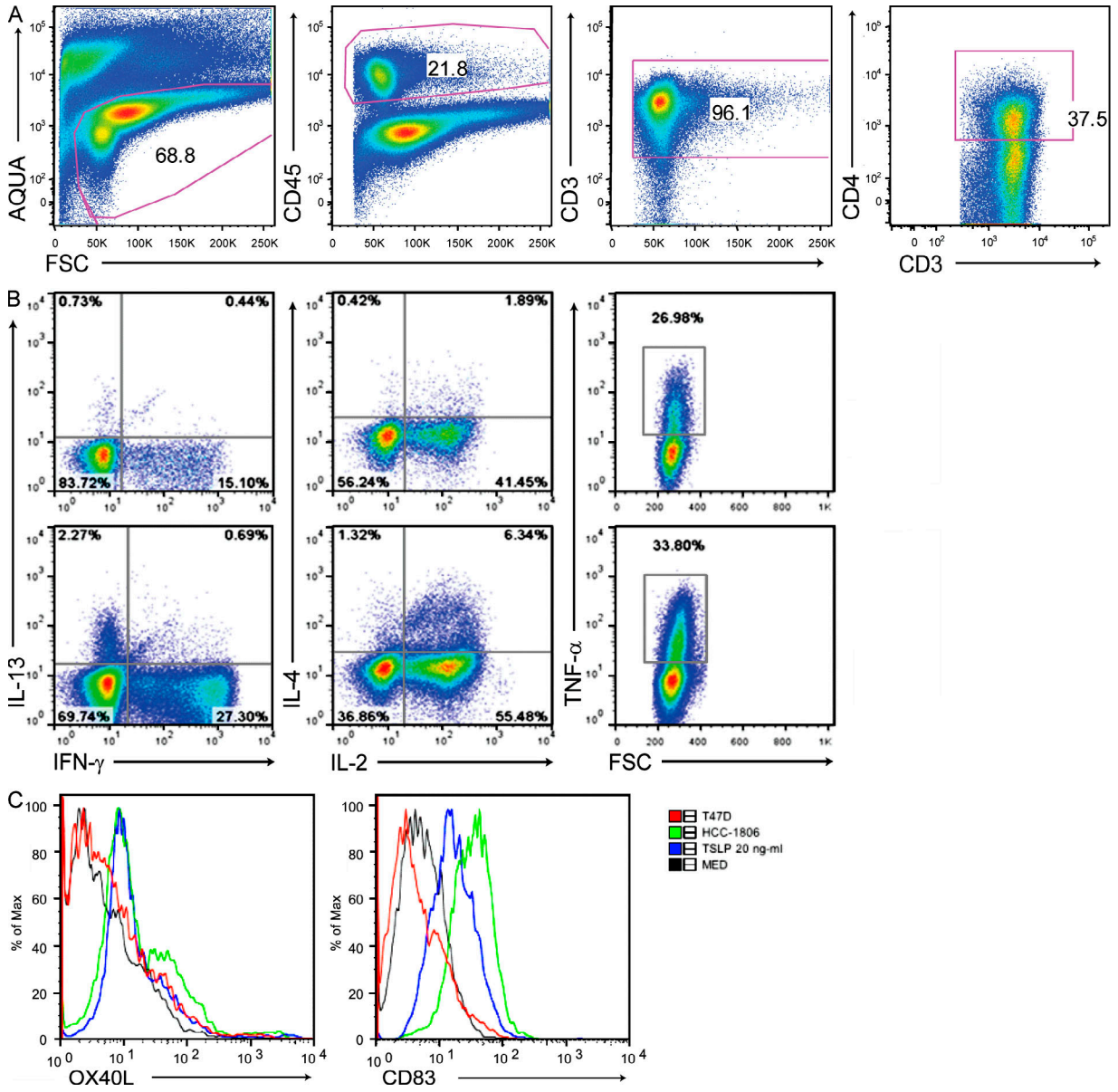

Figure S1. Flow cytometry anlysis of T cells and DCs. (A) Single-cell suspensions from primary human breast tumor samples were obtained by tissue digestion and analyzed by flow cytometry. Viable cells were gated using LIVE/DEAD Fixable Dead Cell Stain kit (Aqua); tumor-infiltrating leukocytes were gated based on CD45 expression. Cytokine production was analyzed in the $CD3^+CD4^+$ T cell gate. (B) As in A, surrounding tissue and tumor cell suspension from the same patient. (C) Blood mDCs were incubated with medium only, with TSLP, or with supernatants from cultured breast cancer cell lines (T47D and HCC-1806). OX40L and CD83 were analyzed by flow cytometry after 48 h.

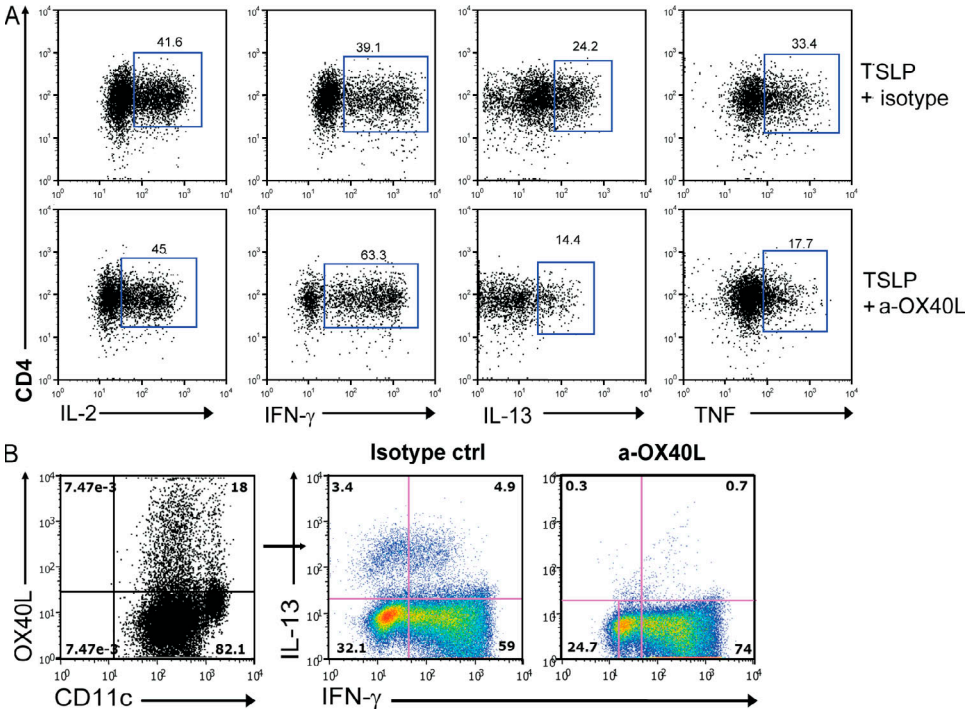

Figure S2. Blockade of OX40L. (A) mDCs were incubated with TSLP for 48 h. Harvested and washed mDCs were then co-cultured with allogeneic naive CD4+ T cells with 40 µg/ml of anti-OX40L or with isotype control antibody for 7 d. Cells were restimulated for 5 h with PMA and ionomycin and analyzed by flow cytometry. Data are representative of four experiments. (B) As in A, but mDCs were incubated with soluble factors from human primary breast tumors. Data from one representative experiment using tumors from three different patients.

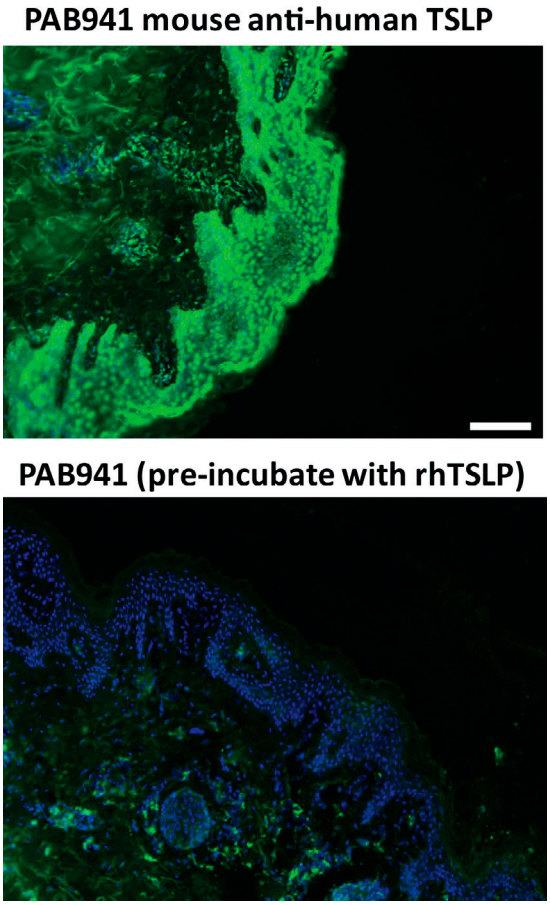

Figure S3. TSLP expression. (top) Frozen sections of human abdominal skin were stained with Alexa Fluor 488–conjugated anti-TSLP at 5 µg/ml. (bottom) Anti-TSLP antibody was preincubated for 1 h at room temperature with recombinant human TSLP (R&D Systems). Bar, 180 µm.

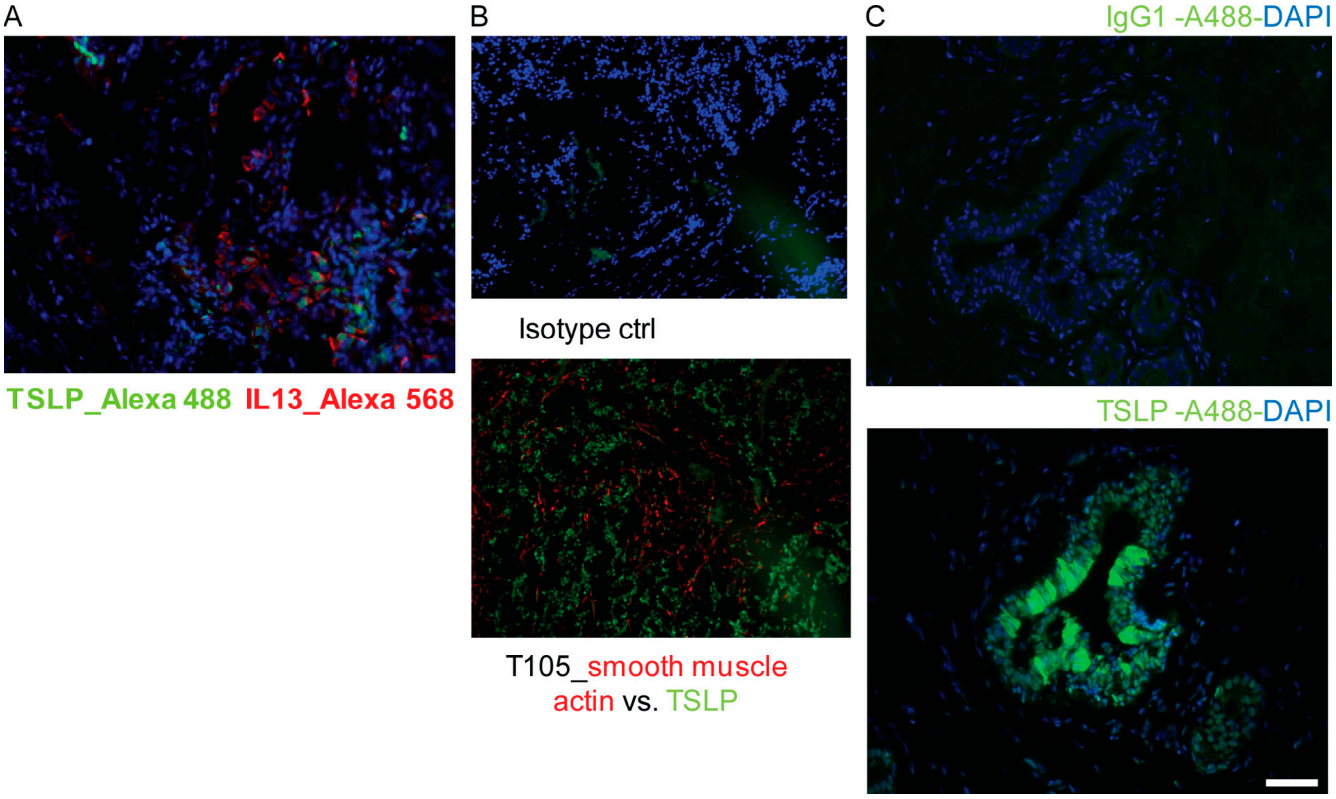

Figure S4. TSLP expression in breast tissues. (A) Frozen section from lung tissue displaying breast metastasis was stained with anti-TSLP (green) and anti–IL-13 (red). Bar, 90 µm. (B) primary breast tumor tissue was stained with anti-TSLP (green) and anti–Smooth Muscle Actin (red; Clone1A4; Invitrogen). Bar, 180 µm. (C) Frozen tissue sections from nonmalignant breast tissues were stained with anti-TSLP followed by goat anti–mouse IgG1 Alexa Fluor 488 (green; Invitrogen). Bar, 900 µm.

Table S2. Cell line characteristics

Cell line	Original Tissue (derived from metastatic site)	Histopathological diagnosis	Receptor status			
			PR	ER	her2	IGF-IR
Hs 578T	Breast	Primary, invasive ductal carcinosarcoma	–	–	low	low
HCC-1806	Breast	Primary, acantholytic squamous carcinoma				+
MDA-MB-231	Breast (pleural effusion)	Metastatic, invasive ductal carcinoma				low
MDA-MB-468	Breast (pleural effusion)	Metastatic, adenocarcinoma				+
MCF7	Breast (pleural effusion)	Metastatic, invasive ductal carcinoma	+	+	low	+
T47D	Breast (pleural effusion)	Metastatic, invasive ductal carcinoma	+	+	+	+

The characteristic of six breast cancer cell lines. Receptor status: ER/PR/IGF-IR positivity, HER2 overexpression is indicated. ER, estrogen receptor; PR, progesterone receptor; HER2, human epidermal growth factor receptor 2; IGF-IR, insulin-like growth factor-I receptor.